
Cost-effective Framework for Gradual Domain Adaptation with Multifidelity

Shogo Sagawa¹ and Hideitsu Hino^{2,3}

¹ Department of Statistical Science, School of Multidisciplinary Sciences, The Graduate University for Advanced Studies (SOKENDAI)

Shonan Village, Hayama, Kanagawa, 240-0193, Japan

²Department of Statistical Modeling, The Institute of Statistical Mathematics
10-3 Midori-cho, Tachikawa, Tokyo, 190-8562, Japan

³Center for Advanced Intelligence Project(AIP), RIKEN,
1-4-4 Nihonbashi, Chuo-ku, Tokyo, 103-0027, Japan

Keywords: **Gradual domain adaptation, Active learning, Multifidelity learning**

Abstract

In domain adaptation, when there is a large distance between the source and target domains, the prediction performance will degrade. Gradual domain adaptation is one of the solutions to such an issue, assuming that we have access to intermediate domains, which shift gradually from the source to target domains. In previous works, it was assumed that the number of samples in the intermediate domains is sufficiently large; hence, self-training was possible without the need for labeled data. If access to an intermediate domain is restricted, self-training will fail. Practically, the cost of samples in intermediate domains will vary, and it is natural to consider that the closer an intermediate domain is to the target domain, the higher the cost of obtaining samples from the intermediate domain is. To solve the trade-off between cost and accuracy, we propose a framework that combines multifidelity and active domain adaptation. The effectiveness of the proposed method is evaluated by experiments with both artificial and real-world datasets. Codes are available at <https://github.com/ssgw320/gdamf>.

1 Introduction

In the standard prediction problems using machine learning models, it is assumed that the test data in operation are samples obtained from the same probability distribution as the training data. It is known that the prediction performance deteriorates when the assumption is broken. The simplest solution is to discard the training data and construct a new machine learning model by collecting new samples obtained from the same probability distribution as the prediction target. However, obtaining enough samples to construct a new machine learning model generally requires a large amount of cost.

Transfer learning [50] is a technique to effectively use of existing data, similarly to human thinking that makes use of past experiences. In transfer learning, when the probability distributions of the training data and the prediction target are different but the task of machine learning is the same, the problem is known as domain adaptation [2]. In domain adaptation, the training data distribution with rich labeled data is called the source domain, and the distribution of the prediction target is called the target domain. The case where a small number of labels are available from the target domain is called semi-supervised domain adaptation [43], and the case where there are no labels at all is called unsupervised domain adaptation [45]. The problem of

unsupervised domain adaptation is more difficult and has been the subject of much research, including theoretical analysis [22, 6, 33, 47].

In domain adaptation, the smaller the distance between the source and target domains, the higher the predictive power for the target data, and the larger the distance between the domains, the lower the predictive power in general. On the other hand, even when the distance between the source and target domains is large, the shift from the source domain to the target domain is assumed to occur gradually, and gradual domain adaptation was proposed in [19]. Gradual domain adaptation has the potential to make it possible to predict data in the target domain that is far different from the source domain by adding data from intermediate domains that interpolate between the source and target pairs.

As an example, we consider the case where a domain shift occurs as time elapsed. Suppose the frequency of coughing is measured, and the purpose of the study is to determine whether people have influenza or not, on the basis of the frequency of coughing. Suppose that the source dataset is sampled in April, the target dataset will be sampled in December, and the intermediate dataset is sampled between May to November. Note that the label is given only for the source dataset (April). Kumar et al. [19] showed that it is possible to predict the target dataset by repeatedly feeding the intermediate dataset (in the order of May to November) to the model trained using the source dataset and self-training with pseudo-labels. This method is unsupervised domain adaptation, which is attractive because it does not need labels for any domain other than the source domain. However, its accuracy is highly dependent on the distance between domains, and in this example, if the frequency of acquisition between intermediate domains is reduced from once a month to every other month, there is a concern that self-training will fail and accuracy will decrease.

The self-training for gradual domain adaptation has limited applicability because the distance between intermediate domains can be large in practical situations. We propose the application of active domain adaptation, which combines domain adaptation with active learning, as a solution to this problem. In reality, each query from each domain comes with some cost, and the cost is not uniform. In domain adaptation, we consider the case that the reason why the target dataset has no label is because of its high cost. Moreover, it is natural to assume that the cost of obtaining data from the intermediate domain is higher when it is closer to the target domain and lower when it is closer to the source domain. To resolve this trade-off between cost and uncertainty, by utilizing the notion of multifidelity learning [27], we propose gradual domain adaptation with multifidelity learning (GDAMF) as an active domain adaptation framework. The features of our proposed method are as follows.

1. Since it is a gradual domain adaptation method, domain adaptation is possible even when the distance between the source and target domains is large.
2. Even when the number of accessible intermediate domains is limited and self-training fails, domain adaptation can be achieved with a small number of efficient queries considering the cost of data acquisition.

The rest of the paper is organized as follows. We review some related works in Section 2, then introduce our proposed method in Section 3. In Section 4, we presents the experiments. We discuss our method in Section 5. Section 6 is devoted to conclusion.

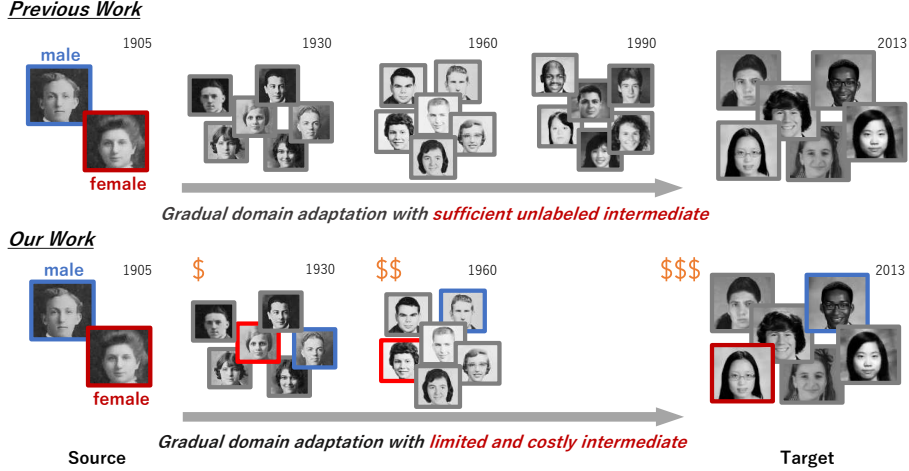


Figure 1: Our problem settings and proposed method with an example of the classification between male and female using portraits. To tackle the gradual domain shift in the situation where access to the intermediate domains is restricted and self-training is not possible, we request a small number of queries with different cost for each domain. A gray frame around the photo indicates that it is unlabeled, while a red or blue one indicates that it is labeled.

2 Related works

2.1 Gradual domain adaptation

In the context of domain adaptation, several methods have been developed to access one intermediate domain to improve the predictive power on the target dataset [16, 5, 7, 8, 12, 10]. In these methods, generative models are used such as generative adversarial networks (GAN) [24] and normalizing flow [25] and the datasets from the source and target domains are mixed at arbitrary ratios to obtain the intermediate dataset. This procedure is regarded as learning common features shared between both the source and target domains. It is assumed in [42] that all intermediate datasets are given as labeled source datasets. The continuous change from the source domain to the target domain is learned under the condition that the source domain is finely partitioned and indices for identifying the intermediate domains are given. We consider a more severe situation than [42], since we have limited access to intermediate domains and labels.

Kumar et al. [19] demonstrated that self-learning domain adaptation is possible under the condition that there is an intermediate domain whose similarity to the source/target domain is known. In addition, theoretical analysis is also performed to show the upper bounds of self-learning. The situation where the intermediate domain exists but the index is unknown is considered in [46, 4], and a method to align the intermediate domain is proposed. In [46], a method to artificially generate datasets with gradual domain change is proposed. In the method, a subset of data with high prediction reliability is sampled from the source dataset and the target dataset in predetermined proportions, and the mixed subsamples are used as an intermediate dataset. Note that this dataset is labeled by the ground-truth label for source-originated data and the predicted label for the target-originated data. The number of updates of the model is given as a hyperparameter, and the percentage of the target dataset is increased as the number of updates increases to represent the gradual change. However, this method does not take full advantage of the gradual domain adaptation setting because of its data generation procedure; the support of data distributions of the source, target, and intermediate domains will have large overlaps. Chen et al. [4] proposed a fine-tuning method to minimize the cycle consistency of self-training by

giving a coarse domain discriminator as the initial guess of the domain index for each datum. It is shown that this method can cope with the case where the index of the intermediate domain is unknown or where data unsuitable for the intermediate domain are included. However, it is also noted that the prediction accuracy decreases significantly when the interval between intermediate domains is large. In [1], the authors consider the situation where there is a large distance between the source and target domains and the intermediate domain is not directly accessible. They propose to mix the source and target data at an arbitrary ratio, and use as the data from the intermediate domain. A possibility of self-learning is also mentioned.

2.2 Active domain adaptation

Active domain adaptation, which combines domain adaptation with active learning, was proposed in [31, 35]. In active domain adaptation, the aim is to obtain a higher predictive power than in the case of using domain adaptation alone by querying the target dataset taking its predictive uncertainty into account. Active domain adaptation has since been extended to deep learning [48, 38]. The querying strategies range from those based on clustering [30] to margins of classifiers. Batch query methods are also proposed in [29, 23].

2.3 Multifidelity learning

Multifidelity learning is a technique that has been developed mainly in the field of simulation to alleviate the problem of high computational cost for obtaining highly accurate simulation results, and its combination to active learning and Bayesian optimization are also considered [20, 39]. Specifically, by combining simulators with various accuracies and costs, it aims to achieve the comparable accuracy and lower costs as those of using only high-accuracy simulators. It is also gaining importance in the relation to the diversity of labelers problem in crowdsourcing [17]. A survey of multifidelity learning can be found in [27]. To construct a model that integrates multiple fidelities in multifidelity learning, studies to improve the representation of correlations between fidelities [21] and have deal with heterogeneous inputs [14, 36] have been conducted. There have also been studies on high-dimensional outputs to handle large-scale simulations [44, 28]. Examples of combining multifidelity learning with Bayesian optimization and active learning have been described in several papers [13, 9, 40], but the acquisition function used does not take into account the correlation and cost between simulators. The acquisition function used is one that determines the sample to be queried by considering the correlation between simulators and cost. Our proposed GDAMF differs in that it uses an acquisition function designed to improve the accuracy of classifications as well as the usual domain adaptation.

In this paper, we consider gradual active domain adaptation, which consists of multiple domains with different query costs. To the best of authors' knowledge, there has been no study on active domain adaptation that queries from multiple domains considering the cost. We note that since the conventional active domain adaptation methods can also be implemented as gradual domain adaptation by sequentially executing them, we conduct experiments to compare the results with those in [31] in Section4.

3 Proposed method

We consider a multiclass classification problem where $x \in \mathbb{R}^{d_1}$ is a feature vector, $y \in \{1, 2, \dots, N\}$ is a class label, and Y is a random variable of y . The neural network is flexible and often used for encoder (feature extractor) for domain adaptation [16, 5, 7, 8, 12, 10]; therefore, we use

neural network encoder in our proposed method GDAMF. The latent variable of \mathbf{x} transformed by the neural network is denoted by $\mathbf{z} \in \mathbb{R}^{d_2}$.

Let $D^{(0)}, D^{(1)}, \dots, D^{(K)}$ be the labeled dataset obtained from each domain. $D^{(0)}$ is the source dataset, $D^{(K)}$ is the target dataset, and the other are intermediate datasets $D^{(j)} := \{(\mathbf{x}_i^{(j)}, y_i^{(j)})\}_{i=1}^{n^{(j)}}$. The subscript i indicates the data, and the superscript (j) indicates the domain. Here, $n^{(j)}$ is the number of labeled data obtained from domain j , where $n^{(j)} \neq 0$, $n^{(0)} \gg n^{(1)}, \dots, n^{(K)}$. Unlabeled pooled datasets $P^{(1)}, P^{(2)}, \dots, P^{(K)}$, $P^{(j)} := \{\mathbf{x}_i^{(j)}\}_{i=1}^{\infty}$ are also available from each domain except source domain. When the queried datum from the pool is annotated, each dataset in domain j is updated as

$$D^{(j)} = D^{(j)} \cup (\mathbf{x}_i^{(j)}, y_i^{(j)}), \quad P^{(j)} = P^{(j)} \setminus \mathbf{x}_i^{(j)}. \quad (1)$$

Each domain has a query cost $c^{(j)} \in \mathbb{R}$, $\mathbf{c} := (c^{(1)}, c^{(2)}, \dots, c^{(K)})$, and if the domain is close to the target, the cost becomes higher, $c^{(1)} < c^{(2)} < \dots < c^{(K)}$. Let $m^{(j)} \in \mathbb{N}$, $\mathbf{m} := (m^{(1)}, m^{(2)}, \dots, m^{(K)})$ be the number of samples to query from the pool dataset in the domain j . The cost \mathbf{c} is given according to the problem, while the number of query samples \mathbf{m} is determined from the dataset as explained later. Finally, there is a pre-fixed budget $B \in \mathbb{R}$, and the total cost cannot exceed the budget, $\mathbf{m} \mathbf{c}^T \leq B$.

In gradual domain adaptation, it is assumed that the similarity between neighboring domains is high. Therefore, we designed GDAMF as a model that takes into account the information between neighboring domains. The overall architecture of GDAMF is shown in Fig. 2. When the domain shift is gradual, the latent variables and class labels between adjacent domains are likely to be similar. Therefore, GDAMF predicts the class labels of the next domain by modifying some of the latent variables and class labels of the previous domain.

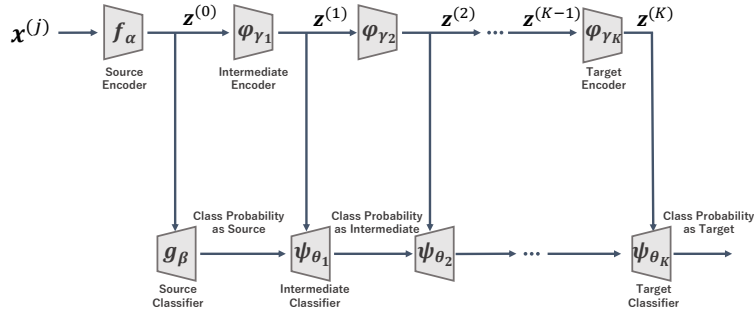


Figure 2: Overall architecture of GDAMF. In the case of a gradual domain shift, the latent variables and class labels between adjacent domains are likely to be similar. GDAMF can effectively use the information of the prior domain to predict the class labels of the next domain. Since the input dimensions of each module are different depending on the source and intermediate/target, the notation of the encoder and classifier is changed.

GDAMF has an encoder and a classifier for each domain and uses the output of the previous domain to predict the next output. The final output from GDAMF is a conditional posterior probability vector $(p_1, p_2, \dots, p_N) \in \Delta_N$ computed using the softmax function [49]. Note that Δ_N is the N -probability simplex, $p_l = \Pr(Y = l | G(E(\mathbf{x})))$, $l = \{1, \dots, N\}$, and $\sum_{l=1}^N p_l = 1$, where G and E indicate a classifier (g or ψ) and an encoder (f or φ), respectively, depending on the context. The encoder and classifier for the source dataset are defined as

$$f_{\alpha} : \mathbb{R}^{d_1} \rightarrow \mathbb{R}^{d_2}$$

$$\mathbf{x} \mapsto \mathbf{z}^{(0)},$$

and

$$\begin{aligned} g_\beta : \mathbb{R}^{d_2} &\rightarrow \Delta_N \\ \mathbf{z}^{(0)} &\mapsto (p_1, p_2, \dots, p_N), \end{aligned}$$

respectively. The q th encoder and classifier for the intermediate and target datasets are defined as

$$\begin{aligned} \varphi_{\gamma_q} : \mathbb{R}^{d_2} &\rightarrow \mathbb{R}^{d_2} \\ \mathbf{z}^{(q-1)} &\mapsto \mathbf{z}^{(q)}, \end{aligned}$$

and

$$\begin{aligned} \psi_{\theta_q} : \mathbb{R}^{d_2} \times \Delta_N &\rightarrow \Delta_N \\ (\mathbf{z}^{(q)}, M'_{q-1}(\mathbf{x})) &\mapsto (p_1, p_2, \dots, p_N), \end{aligned}$$

respectively. Note that the input dimensions are different for the encoder and classifier for the source (f_α, g_β) and intermediate/target $(\varphi_{\gamma_q}, \psi_{\theta_q})$. We defined $M'_q : \mathbb{R}^{d_1} \ni \mathbf{x} \mapsto (p_1, p_2, \dots, p_N) \in \Delta_N$ inductively as follows.

$$M'_q(\mathbf{x}) = \begin{cases} g_\beta \circ f_\alpha(\mathbf{x}) & q = 0 \\ \psi_{\theta_q}(\mathbf{z}^{(q)}, M'_{q-1}(\mathbf{x})) & q \neq 0, \end{cases} \quad (2)$$

where α, β, γ_q , and θ_q are the parameters for the encoder and classifier.

We define a composite map consisting of $f_\alpha, g_\beta, \varphi_{\gamma_q}, \psi_{\theta_q}$, $q = 1, \dots, K$ as GDAMF:

$$\begin{aligned} M_{\alpha, \beta, \{\gamma_q, \theta_q\}_{q=1}^K} : \mathbb{R}^{d_1} &\rightarrow \Delta_N \\ \mathbf{x} &\mapsto (p_1, p_2, \dots, p_N). \end{aligned} \quad (3)$$

In the case of $K = 0$, GDAMF is nothing but the function $M_{\alpha, \beta}$ composed of f_α and g_β . In the case of $K = 2$, GDAMF is a function $M_{\alpha, \beta, \gamma_1, \gamma_2, \theta_1, \theta_2}$ composed of $f_\alpha, g_\beta, \varphi_{\gamma_1}, \psi_{\theta_1}, \varphi_{\gamma_2}$, and ψ_{θ_2} . Depending on the domain j of the input \mathbf{x} , the output of GDAMF changes as

$$M_{\alpha, \beta, \{\gamma_q, \theta_q\}_{q=1}^K}(\mathbf{x}^{(j)}) = \begin{cases} g_\beta \circ f_\alpha(\mathbf{x}^{(j)}) & j = 0, \\ \psi_{\theta_j}(\varphi_{\gamma_j} \circ \dots \circ \varphi_{\gamma_1} \circ f_\alpha(\mathbf{x}^{(j)}), M'_{j-1}(\mathbf{x}^{(j)})) & j = 1, 2, \dots, K. \end{cases}$$

GDAMF has a module for each domain, and we try to minimize the loss for all domains. Using softmax function and indicator function $\mathbb{1}$, we define the loss functions as follows:

$$J(\alpha, \beta, \{\gamma_q, \theta_q\}_{q=1}^K; \{D^{(j)}\}_{j=0}^K) = - \sum_{j=0}^K \frac{1}{n^{(j)}} \sum_{(\mathbf{x}_i^{(j)}, y_i^{(j)}) \in D^{(j)}} \sum_{l=1}^N \mathbb{1}\{y_i^{(j)} = l\} M_{\alpha, \beta, \{\gamma_q, \theta_q\}_{q=1}^K}(\mathbf{x}_i^{(j)}). \quad (4)$$

Since the labeled data from the intermediate and target domains are limited, it is unlikely that we can obtain an accurate model from this alone. Therefore, we aim to use active learning with the gradual domain adaptation, and require a small amount of queries to obtain a model with good accuracy. The minimization of Eq. (4) is performed on the initial datasets and on the datasets collected by active learning. In the usual active domain adaptation, since the query object is only the target domain, we can execute queries from the pooled dataset of the target domain until the budget is used up. On the other hand, we consider the situation of multifidelity

learning, where multiple domains exist for gradual domain adaptation and each domain has its own acquisition cost. In this case, if we focus on queries from the pooled data in the domain, which are useful for predicting the target, the budget will be exhausted immediately, we will not obtain sufficient amount of data to train a good model for the target domain.

On the basis of the multifidelity Monte Carlo method [26, 27], we considered the optimization of the number of query samples \mathbf{m} in each domain by distributing budgets considering cost and fidelity. See also Algorithm1 for an overview of multifidelity active learning. For the optimal distribution of budgets, we first calculate $\mathbf{r} = (r^{(1)}, r^{(2)}, \dots, r^{(K-1)}, r^{(K)})$ where $r^{(s)}$ is defined as follows:

$$r^{(s)} = \sqrt{\frac{c^{(K)}(\rho_s^2 - \rho_{s-1}^2)}{c^{(s)}(1 - \rho_{K-1}^2)}}, \quad s = 1, \dots, K-1, \quad (5)$$

where ρ_s is the correlation coefficient between the output of the function $M_{\alpha, \beta, \{\gamma_q, \theta_q\}_{q=1}^K}(\mathbf{u})$ for the prediction of $\mathbf{x}^{(K)}$ and the output of the function $M_{\alpha, \beta, \{\gamma_q, \theta_q\}_{q=1}^j}(\mathbf{u})$ for the prediction of $\mathbf{x}^{(j)}$. Note that to evaluate ρ_s , we sampled the output of the function $M_{\alpha, \beta, \{\gamma_q, \theta_q\}_{q=1}^j}(\mathbf{u})$ by inputting randomly sampled $\mathbf{u} \in \mathbb{R}^{d_1}$. Each element of the sample \mathbf{u} is uniformly chosen from the range of the observed maximum and minimum values of the original input data \mathbf{x}_i in element-wise manner. When $s = 1$, $\rho_{s-1} = 0$. In the original multifidelity Monte Carlo method, $r^{(K)} = 1$, but we consider a situation where the cost of the target is very high; thus, we set $r^{(K)} = 0.1$ to reduce the number of queries from the target domain. From the budget and the calculated \mathbf{r} , the optimal number of queries $m^{(K)}$ from target domain is obtained by

$$\tilde{m}^{(K)} = \frac{B}{\mathbf{r} \mathbf{c}^T}. \quad (6)$$

Using $\tilde{m}^{(K)}$, we calculate the number of queries from other domains by

$$\tilde{m}^{(s)} = r^{(s)} \tilde{m}^{(K)}, \quad s = 1, \dots, K-1. \quad (7)$$

We round down $\tilde{m}^{(1)}, \tilde{m}^{(2)}, \dots, \tilde{m}^{(K)}$ to obtain an integer number and denote the optimal number of queries \mathbf{m}

$$\mathbf{m} = (m^{(1)}, m^{(2)}, \dots, m^{(K)}) = (\lfloor \tilde{m}^{(1)} \rfloor, \lfloor \tilde{m}^{(2)} \rfloor, \dots, \lfloor \tilde{m}^{(K)} \rfloor). \quad (8)$$

Next, we add labels by active learning for the number of samples obtained from each domain $m^{(j)}$. The samples to be queried are determined on the basis of uncertainty [32], which is a standard measure in active learning [37, 15]. Since GDAMF retain the data of all domains, so the network tends to be huge. To alleviate computational difficulty, we introduce mini-model for each domain, and repeat uncertainty calculation, query and model update for each mini-model. Let $h_{\omega_j} : \mathbf{x}^{(j)} \mapsto (p_1, p_2, \dots, p_N)$ be the mini-model of each domain, and trained by minimizing the following loss function for each step in active learning.

$$J_{\text{mini}}(\omega_j; D^{(j)}) = -\frac{1}{n^{(j)}} \sum_{(\mathbf{x}_i^{(j)}, y_i^{(j)}) \in D^{(j)}} \sum_{l=1}^N \mathbb{1}\{y_i^{(j)} = l\} h_{\omega_j}(\mathbf{x}_i^{(j)}). \quad (9)$$

With the trained mini-model h_{ω_j} , we compute the uncertainty of the samples in the pooled dataset $P^{(j)}$ of domain j and query for the datum $x^{(j)*}$ with the largest uncertainty.

$$\text{unc}(\mathbf{x}_i^{(j)}) = 1 - \max_{l \in \{1, \dots, N\}} \Pr(Y = l | h_{\omega_j}(\mathbf{x}_i^{(j)})), \quad (10)$$

$$\mathbf{x}^{(j)*} = \underset{\mathbf{x}_i^{(j)} \in P^{(j)}}{\text{argmax}} \text{unc}(\mathbf{x}_i^{(j)}). \quad (11)$$

The queried $\mathbf{x}^{(j)*}$ is excluded from $P^{(j)}$ and added to $D^{(j)}$ with its label. Then we update the mini model with the new $D^{(j)}$ and Eq. (9). This operation is repeated $m^{(j)}$ times.

Algorithm 1 Gradual Domain Adaptation with Multifidelity Active Learning

Input: initial data set $D^{(0)}, \dots, D^{(K)}$, budget B , cost \mathbf{c}

Output: trained model $M_{\alpha, \beta, \{\gamma_q, \theta_q\}_{q=1}^K}$, updated datasets $D^{(0)}, \dots, D^{(K)}$

- 1: train $M_{\alpha, \beta, \{\gamma_q, \theta_q\}_{q=1}^K}$ with initial labeled datasets $D^{(0)}, \dots, D^{(K)}$ by minimization of Eq. (4)
- 2: compute $\rho_1, \rho_2, \dots, \rho_{K-1}$
- 3: compute \mathbf{r} by solving Eq. (5)
- 4: compute optimal number of queries from each pool dataset \mathbf{m} by solving Eq. (8)
- 5: **for each** $j \in \{1, 2, \dots, K\}$ **do**
- 6: **for** $c = 1$ to $m^{(j)}$ **do**
- 7: train mini model h_{ω_j} with $D^{(j)}$ by minimization of Eq. (9)
- 8: compute uncertainty by solving Eq. (10)
- 9: select query datum $x^{(j)*}$ by solving Eq. (11)
- 10: query label of $x^{(j)*}$, and obtain $y^{(j)*}$
- 11: update labeled and unlabeled dataset by using Eq. (1)
- 12: $c \leftarrow c + 1$
- 13: **end for**
- 14: **end for**
- 15: train $M_{\alpha, \beta, \{\gamma_q, \theta_q\}_{q=1}^K}$ with updated labeled datasets $D^{(0)}, \dots, D^{(K)}$ by minimization of Eq. (4)

4 Experiments

4.1 Datasets

We will modify existing data sets to emulate a gradual domain shift situation. Most of the datasets used in this paper are adopted from existing works [19, 1]. We also add a gas sensor dataset [41, 34], which is considered more realistic gradual domain adaptation datasets.

Rotating moon (toy data): We prepared two-moon dataset as the source dataset, and consider its rotated version as intermediate and target datasets. There were four intermediate datasets in total, with rotation angles of $j \times \pi/10$, $j = 1, \dots, 4$. The target dataset is the one rotated by $\pi/2$. The number of data from each domain was 2000, and since it was a toy dataset, an independently sampled dataset from the target domain was used as the evaluation dataset. A similar experiment has been carried out in [1].

Rotating MNIST: We prepared the rotating MNIST datasets, following a previous work [19]. We prepared 2000 source datasets with randomly added rotations of $0 - \pi/36$, 42000 intermediate dataset with added gradually rotations of $\pi/36 - \pi/3$, and 2000 target and evaluation datasets with randomly added rotations of $\pi/3.27 - \pi/3$. The intermediate dataset was divided into 21 parts.

Portraits: A dataset of actual photos of American high school students taken from 1905 to 2013 was used, and the task was to guess the gender from the images [11]. We prepared the portraits dataset following a previous work [19]; the dataset was sorted in ascending order by year, with source, intermediate, target, and evaluation datasets beginning with the oldest. All datasets had 1000 data each, and the intermediate had 14 domains in total.

Cover type: Cover type is a dataset available from the UCI repository. The task was to guess the type of plants in a group from 54 features [3]. Following the previous work [19], we consider the binary classification problem by extracting only Spruce/Fir and Lodgepole Pine, which are the majority of the seven objective variables. In descending order of distance from the water body, the source, intermediate, target, and evaluation datasets were created. There are 30 intermediate domains in total, and each datasets had 10000 samples.

Gas sensor: Gas sensor dataset is available from the UCI repository. The task was to guess the type of chemical from the responses of 128 sensors [41, 34]. The data were divided into batches along the time the gas were processed, and shifts occurred as the sensor degraded along the batches. Although the original objective variables were six (Ethanol, Ethylene, Ammonia, Acetaldehyde, Acetone, and Toluene), there was a period when no Toluene was observed. It was merged with Acetaldehyde, for which a similar sensor response was obtained, to obtain five objective variables. The last 3600 data were excluded because they were measured in very different environments. See [41] for details. In ascending order of batch, the source, intermediate, target, and evaluation datasets were used. All datasets have 1000 data each, and the intermediate had 7 domains in total.

4.2 Experimental settings

In the case of the rotating MNIST and portraits datasets, the classifier network f_α was composed of three convolutional layers, one dropout, and one batch normalization layers. The encoder network φ_{γ_j} was composed of one fully connected layer, dropout, and batch normalization layers. In other four datasets, f_α and φ_{γ_j} were composed of one fully connected layer, dropout, and batch normalization layers. The encoder of the mini model used for active learning had the same network configuration as that of f_α . We used Adam [18] as the optimizer, and the learning rate and weight decay were both set to 0.001. We set the number of minibatch as 128. In Section 4.4, the number of epochs is set to 100 because there are many intermediate domains, and in the other sections, the number of epochs is set to 50. The results of five repetitions are shown for each experiment.

4.3 Effect of gradual domain adaptation

GDAMF is designed for gradual domain adaptation and expected to utilize the information of both source and intermediate domains to learn a predictive model for the target domain. Figure 3 shows the comparison of the accuracies achieved by GDAMF and learning with the target dataset only, using rotating moon and gas sensor datasets. The vertical axis is the accuracy when the evaluation dataset is predicted by the GDAMF after training. The horizontal axis shows the number of samples $n^{(j)}$, $j = 1, \dots, K$ from the intermediate and target domains in the case of GDAMF, and the number of samples from the target domain $n^{(K)}$ in the case of “target only”. GDAMF always uses the source dataset $D^{(0)}$ for training, and each plot shows an increasing number of samples $n^{(j)}$, $j = 1, \dots, K$ from the intermediate and target domains. In both cases, sampling is random. For both the rotating moon and gas sensor datasets, GDAMF has a higher accuracy than “target only”. In both cases, the number of samples from the target domain $n^{(K)}$ is equal; however, GDAMF has more data by the amount of samples from the

source and intermediate domains $n^{(j)}$, $j = 0, \dots, K - 1$. Although the total number of samples increases in the case of GDAMF, by utilizing source and intermediate domain information, we can obtain better performance than when using only the target dataset.

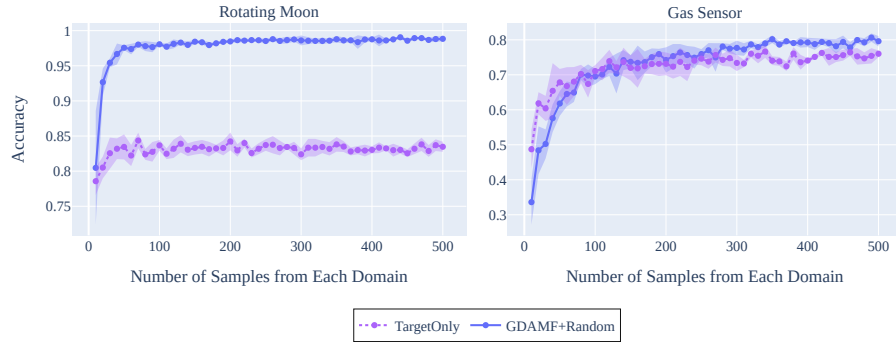


Figure 3: Comparison of the accuracies achieved by GDAMF and model trained the target dataset only. The horizontal axis shows the number of samples from the intermediate and target domains in the case of GDAMF. In this experiment, rotating moon (toy data) and gas sensor datasets were used, both of which confirm the superiority of GDAMF.

4.4 Self-training vs query label

We assume a more realistic case of gradual domain adaptation where access to the intermediate domain is restricted. In this case, the self-training method (GradualSelfTrain) proposed by Kumar et al. [19] will fail, and gradual domain adaptation is also assumed to fail. The problem is addressed by considering semi-supervised domain adaptation instead of unsupervised domain adaptation. Although labeling is burdensome, we reduce this burden by using multifidelity active learning. Experimental setting of the multifidelity active learning is discussed in detail in the next section.

In this section, we show that GDAMF works even when access to the intermediate domain is restricted. Figure 4 shows the results of the comparison between GDAMF and GradualSelfTrain using the rotating MNIST dataset. The vertical axis is the accuracy when the evaluation dataset is predicted after training the model. The horizontal axis shows the number of accessible intermediate domains. In addition, the source and target domains are always accessible. For example, when the horizontal axis is 3, GDAMF and GradualSelfTrain are trained using the source and target datasets ($D^{(0)}$ and $D^{(K)}$) and three randomly selected intermediate datasets (Ex, $D^{(1)}$, $D^{(10)}$, and $D^{(18)}$). In addition to the labeled source dataset $D^{(0)}$, GDAMF obtains a random sample of 200 data $n^{(j)} = 200$ each from domains other than the source. On the other hand, in GradualSelfTrain, label information is only available in the source dataset. Note that the index of the selected intermediate domain (in relation to the Source/Target domain) is assumed to be known.

It is seen from Fig. 4 that if GradualSelfTrain does not have access to a sufficient number of intermediate domains, its self-training fails and gradual domain adaptation also fails. On the other hand, GDAMF can perform gradual domain adaptation even when access to the intermediate domain is restricted.

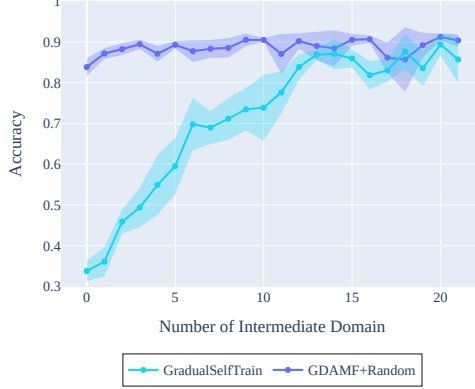


Figure 4: GDAMF works by querying a small number of labels even in situations where self-training fails owing to the limited number of accessible intermediate domains. When the number of accessible intermediate domains is limited, GradualSelfTrain shows a decrease in accuracy, but GDAMF makes excellent predictions in all cases. The accessible intermediate domains were randomly selected.

4.5 Multifidelity active learning

As mentioned in Section 4.4, we performed a small amount of querying to solve the situation where only a restricted number of intermediate domains are accessible in gradual domain adaptation. As a more realistic setting, we consider a situation where each domain has a query cost; the target domain has the highest cost, and the intermediate domain costs higher as it gets closer to the target. Using the method shown in Algorithm 1, we set the number of queries from each domain by considering cost and correlation (fidelity).

We first show how the number of queries from each domain changes with multifidelity active learning. We set 3080 as a sufficient amount of budget for all data sets, and the cost for annotating a datum in domain $D^{(j)}$ is set to j^2 . The cost of the target domain is set to 50 (we are considering a situation where the acquisition cost of the target domain is very high). For example, when the number of intermediate domains is three, the acquisition costs for intermediate domains are 1, 4, and 9, and that for the target domain is 50.

We will not use all of the intermediate domains prepared in Section 4.1, but we will limit to those that can be accessed because the distance between intermediate domains can be large in practical situations. In the rotating MNIST dataset, only the 5th, 10th, and 15th intermediate domains are accessible out of the total 21 intermediate domains. In the portraits dataset, only the 4th, 8th, and 12th intermediate domains are accessible among the total 14 intermediate domains. In the cover type dataset, only the 10th and 20th intermediate domains are accessible among the total 30 intermediate domains. In the gas sensor dataset, only the 2nd, 4th, and 6th intermediate domains are accessible among the total of 7 intermediate domains. From the intermediate and target domains, we sample 20 data each as the initial dataset to find the optimal number of query samples m using Algorithm 1.

The results of the comparison between random sampling and multifidelity active learning are shown in Fig. 5. In all datasets, the number of samples is roughly the same among domains for random sampling, but for multifidelity active learning, the number of samples from each domain varies, considering the correlation (fidelity) with the target domain and the cost. In particular, for portraits and cover type datasets, the distance between source and target domain is expected to be close (see also Table 1), and sampling from the intermediate domain close to the source is preferred because of its high fidelity and low cost.

By combining GDAMF with multifidelity active learning, we can obtain higher accuracy with smaller budget than the combination of GDAMF and random sampling, even when the number of samples from costly domains (target and intermediate near target) is limited. Figure 6 shows the results of comparing the budget required to exceed a given accuracy for each dataset between random sampling and multifidelity active learning. The accuracy thresholds set for each dataset are 0.65 for rotating MNIST, 0.84 for portraits, 0.70 for the cover type, and 0.62 for the gas sensor. In all datasets, multifidelity active learning achieves good accuracy with smaller budget by limiting sampling from costly domains to only those that are useful for modeling.

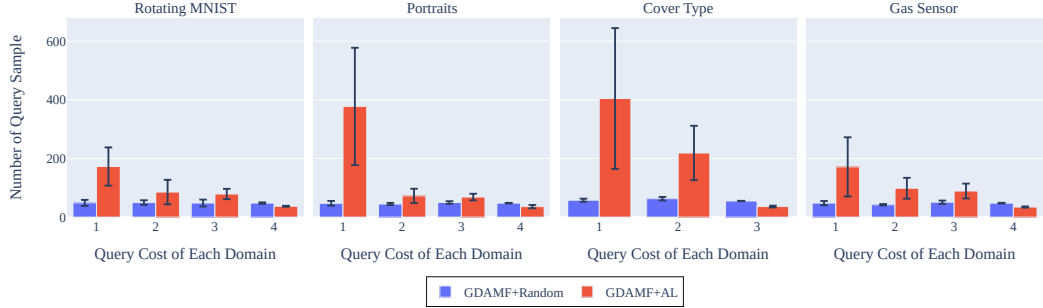


Figure 5: In GDAMF+AL, multifidelity active learning is applied to determine the optimal number of samples from each domain m , considering cost and fidelity. For all datasets, the number of samples from each domain is uniform in GDAMF+Random, whereas the that number of samples varies for each domain in GDAMF+AL.

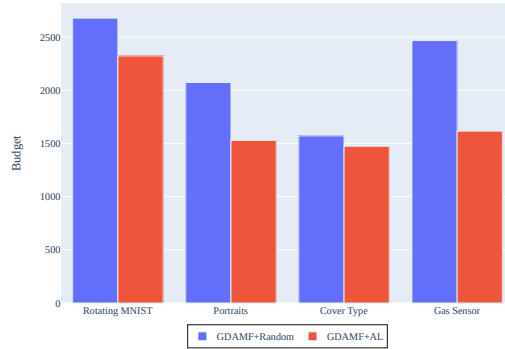


Figure 6: Budget required to exceed the accuracy threshold set for each dataset. GDAMF+AL requires a smaller budget to achieve the same accuracy then GDAMF+Random because it selects useful samples for prediction.

4.6 Comparison with baseline method

Finally, we show that GDAMF can make more accurate predictions with smaller budget than existing baseline methods. DS-AODA [31], which is a previous work on active domain adaptation, is not a method for gradual domain adaptation, but it was used for comparison by updating the model step by step. We include GradualSelfTrain [19], GIFT [1] and AuxSelfTrain [46] in the comparative study because the implementations are publicly available.

The encoder g_β and classifier f_α for each baseline method have the same network configuration as that for the source dataset in GDAMF. The setting of the accessible intermediate domain

for each dataset is the same as that described in Section 4.5. DS-AODA requires the probability of querying, whereas GIFT and AuxSelfTrain require the number of intermediate domains between the source and the target to be assumed as hyper parameters. Three levels, low, mid, and high, were evaluated for these hyperparameters.

Figure 7 shows the results of the comparison between GDAMF and the baseline method with the budget varied for each dataset. For DS-AODA, GIFT, and AuxSelfTrain, only the results for the hyper parameter with the best accuracy are shown. Table 1 shows the comparison results of all the methods for the two cases of small budget and abundant budget. The experimental setup for each baseline method is shown below.

- **Source only:** Train only on the source dataset. It does not depend on budget.
- **Target only:** Random sampling from the target domain for a fixed budget.
- **GDAMF+Random:** Proposed method. Random sampling from target and intermediate domains is performed for a set budget.
- **GDAMF+AL:** Proposed method. It calculates the optimal number of queries from each domain and performs multifidelity active learning for each domain.
- **DS-AODA[31]:** Update the model by querying the neighboring domains in order from source to target domains. The process ends when the budget is exhausted.
- **GradualSelfTrain[19]:** Updates the model by self-training, giving intermediates in order from source to target domains. It does not depend on the budget.
- **GIFT[1]:** This method does not require intermediate domains; only source and target domains are given for training. It does not depend on the budget.
- **AuxSelfTrain[46]:** The intermediate and target domains are merged into a single target domain, and the source and target domains are given for training. It does not depend on the budget.

As can be seen from the “source only” results, the rotating MNIST and gas sensor datasets are particularly difficult tasks for domain adaptation owing to the large distance between the source and target domains. When the number of accessible intermediate domains is restricted in such a dataset, gradual domain adaptation by self-training, such as GradualSelfTrain, shows significant degradation in prediction performance. On the other hand, GDAMF shows the comparable or better performance than the “target only” model on all datasets, indicating that GDAMF is effective when access to intermediate domains is restricted and the cost is set for each domain. Although there are no single method consistently outperform others, the proposed GDAMF stably achieves reasonable results and could be a strong candidate for the active gradual domain adaptation under multifidelity setting.

5 Discussion

It is experimentally shown that the proposed GDAMF can effectively use the information of the intermediate domains; thus, it is possible to predict the target domain only by querying a small number of labels. GDAMF is particularly effective in situations where access to an intermediate domain is restricted hence self-training fails. On the other hand, GDAMF tries to retain the information of all domains, so the network tends to be huge. When there are many accessible

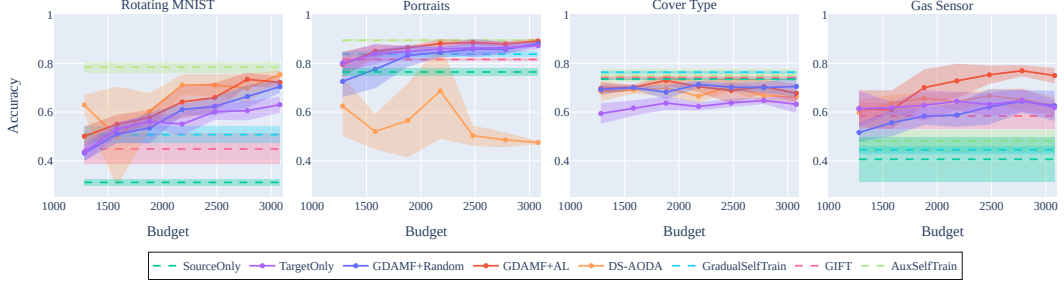


Figure 7: For each dataset, we compared GDAMF with the baseline method with the budget varied. Rotating MNIST and gas sensor dataset show poor results for “source only”, indicating that they are particularly difficult tasks. GDAMF has shown consistently high performance on all datasets.

Table 1: Performances of the proposed method and the baseline methods in the cases of small budget and large budget. The best performing method for each dataset and budget condition is shown in bold. GDAMF has shown comparable performance on all datasets. See Fig. 7 for details of the change in accuracy with respect to budget.

Dataset	Rotating MNIST		Portraits		Cover Type		Gas Sensor	
	Budget	1580	2780	1580	2780	1580	2780	1580
Source Only	0.312 ± 0.013	0.312 ± 0.013	0.764 ± 0.015	0.764 ± 0.015	0.735 ± 0.004	0.735 ± 0.004	0.406 ± 0.092	0.406 ± 0.092
Target only	0.53 ± 0.031	0.605 ± 0.039	0.839 ± 0.042	0.864 ± 0.025	0.616 ± 0.031	0.648 ± 0.014	0.618 ± 0.024	0.647 ± 0.048
GDAMF+Random	0.51 ± 0.037	0.664 ± 0.046	0.775 ± 0.078	0.857 ± 0.017	0.7 ± 0.008	0.7 ± 0.023	0.556 ± 0.055	0.644 ± 0.045
GDAMF+AL	0.55 ± 0.04	0.734 ± 0.028	0.849 ± 0.028	0.879 ± 0.011	0.702 ± 0.012	0.704 ± 0.029	0.609 ± 0.08	0.769 ± 0.023
DS-AODA high	0.499 ± 0.205	0.697 ± 0.061	0.555 ± 0.039	0.534 ± 0.029	0.671 ± 0.009	0.681 ± 0.011	0.636 ± 0.034	0.652 ± 0.046
DS-AODA mid	0.551 ± 0.126	0.437 ± 0.228	0.52 ± 0.073	0.486 ± 0.03	0.665 ± 0.025	0.661 ± 0.02	0.51 ± 0.035	0.535 ± 0.075
DS-AODA low	0.566 ± 0.055	0.665 ± 0.051	0.495 ± 0.051	0.521 ± 0.11	0.69 ± 0.014	0.667 ± 0.031	0.526 ± 0.07	0.569 ± 0.058
GradualSelfTrain	0.507 ± 0.033	0.507 ± 0.033	0.838 ± 0.011	0.838 ± 0.011	0.764 ± 0.004	0.764 ± 0.004	0.446 ± 0.016	0.446 ± 0.016
GIFT high	0.448 ± 0.063	0.448 ± 0.063	0.816 ± 0.005	0.816 ± 0.005	0.728 ± 0.015	0.728 ± 0.015	0.479 ± 0.049	0.479 ± 0.049
GIFT mid	0.394 ± 0.028	0.394 ± 0.028	0.793 ± 0.01	0.793 ± 0.01	0.718 ± 0.006	0.718 ± 0.006	0.497 ± 0.034	0.497 ± 0.034
GIFT low	0.364 ± 0.016	0.364 ± 0.016	0.798 ± 0.016	0.798 ± 0.016	0.74 ± 0.007	0.74 ± 0.007	0.584 ± 0.053	0.584 ± 0.053
AuxSelfTrain high	0.747 ± 0.007	0.747 ± 0.007	0.888 ± 0.006	0.888 ± 0.006	0.743 ± 0.012	0.743 ± 0.012	0.468 ± 0.036	0.468 ± 0.036
AuxSelfTrain mid	0.784 ± 0.022	0.784 ± 0.022	0.879 ± 0.004	0.879 ± 0.004	0.729 ± 0.035	0.729 ± 0.035	0.481 ± 0.044	0.481 ± 0.044
AuxSelfTrain low	0.751 ± 0.007	0.751 ± 0.007	0.895 ± 0.006	0.895 ± 0.006	0.75 ± 0.026	0.75 ± 0.026	0.461 ± 0.025	0.461 ± 0.025

intermediate domains, this tendency becomes more pronounced, and a large number of samples are required to converge the training of a huge neural network. If the number of accessible intermediate domains is sufficiently large, GDAMF is not suitable. On the other hand, gradual domain adaptation by self-training is likely to be successful in such a case [19, 4].

6 Conclusion

In gradual domain adaptation, the existence of an intermediate domain that gradually shifts from the source to the target domain is assumed. We consider the situation where the accessible intermediate domains are restricted, and propose GDAMF. By combining multifidelity and active domain adaptation, we addressed the trade-off between the query cost from each domain and the prediction accuracy using GDAMF. The effectiveness of the proposed method was evaluated on one artificial and four real-world datasets, and it was shown that GDAMF provides reasonable performance under the condition that access to the intermediate domain is restricted and the query cost should be considered.

For future works, we consider it is important to make GDAMF more scalable. By doing so, we expect reducing the number of samples required for convergence of the network, and enable more efficient active learning without introducing the mini-model. Moreover, it is of great importance to theoretically analyze and give guarantee for the effectiveness of the use of

data in intermediate domains.

7 Acknowledgments

H.H. is partly supported by JST CREST Grant Nos. JPMJCR1761 and JPMJCR2015, JST-Mirai Program Grant No. JPMJMI19G1, and NEDO Grant No. JPNP18002.

References

- [1] Abnar, S., Berg, R.v.d., Ghiasi, G., Dehghani, M., Kalchbrenner, N., Sedghi, H.: Gradual domain adaptation in the wild: When intermediate distributions are absent. arXiv preprint arXiv:2106.06080 (2021)
- [2] Ben-David, S., Blitzer, J., Crammer, K., Pereira, F., et al.: Analysis of representations for domain adaptation. *Advances in neural information processing systems* **19**, 137 (2007)
- [3] Blackard, J.A., Dean, D.J.: Comparative accuracies of artificial neural networks and discriminant analysis in predicting forest cover types from cartographic variables. *Computers and electronics in agriculture* **24**(3), 131–151 (1999)
- [4] Chen, H.Y., Chao, W.L.: Gradual domain adaptation without indexed intermediate domains. *Advances in Neural Information Processing Systems* **34** (2021)
- [5] Choi, J., Choi, Y., Kim, J., Chang, J., Kwon, I., Gwon, Y., Min, S.: Visual domain adaptation by consensus-based transfer to intermediate domain. In: *Proceedings of the AAAI Conference on Artificial Intelligence*, vol. 34, pp. 10,655–10,662 (2020)
- [6] Cortes, C., Mansour, Y., Mohri, M.: Learning bounds for importance weighting. In: *Nips*, vol. 10, pp. 442–450. Citeseer (2010)
- [7] Cui, S., Wang, S., Zhuo, J., Su, C., Huang, Q., Tian, Q.: Gradually vanishing bridge for adversarial domain adaptation. In: *Proceedings of the IEEE/CVF Conference on Computer Vision and Pattern Recognition*, pp. 12,455–12,464 (2020)
- [8] Dai, Y., Liu, J., Sun, Y., Tong, Z., Zhang, C., Duan, L.Y.: Idm: An intermediate domain module for domain adaptive person re-id. In: *Proceedings of the IEEE/CVF International Conference on Computer Vision*, pp. 11,864–11,874 (2021)
- [9] Dhulipala, S., Shields, M., Spencer, B., Bolisetti, C., Slaughter, A., Laboure, V., Chakraborty, P.: Active learning with multifidelity modeling for efficient rare event simulation. arXiv preprint arXiv:2106.13790 (2021)
- [10] Gadermayr, M., Eschweiler, D., Klinkhammer, B.M., Boor, P., Merhof, D.: Gradual domain adaptation for segmenting whole slide images showing pathological variability. In: *International Conference on Image and Signal Processing*, pp. 461–469. Springer (2018)
- [11] Ginosar, S., Rakelly, K., Sachs, S., Yin, B., Efros, A.A.: A century of portraits: A visual historical record of american high school yearbooks. In: *Proceedings of the IEEE International Conference on Computer Vision Workshops*, pp. 1–7 (2015)
- [12] Gong, R., Li, W., Chen, Y., Gool, L.V.: Dlow: Domain flow for adaptation and generalization. In: *Proceedings of the IEEE/CVF Conference on Computer Vision and Pattern Recognition*, pp. 2477–2486 (2019)

- [13] Grassi, F., Manganini, G., Garraffa, M., Mainini, L.: Resource aware multifidelity active learning for efficient optimization. In: AIAA Scitech 2021 Forum, p. 0894 (2021)
- [14] Hebbal, A., Brevault, L., Balesdent, M., Talbi, E.G., Melab, N.: Multi-fidelity modeling with different input domain definitions using deep gaussian processes. *Structural and Multidisciplinary Optimization* **63**(5), 2267–2288 (2021)
- [15] Hino, H.: Active learning: Problem settings and recent developments. *CoRR* **abs/2012.04225** (2020). URL <https://arxiv.org/abs/2012.04225>
- [16] Hsu, H.K., Yao, C.H., Tsai, Y.H., Hung, W.C., Tseng, H.Y., Singh, M., Yang, M.H.: Progressive domain adaptation for object detection. In: Proceedings of the IEEE/CVF Winter Conference on Applications of Computer Vision, pp. 749–757 (2020)
- [17] Huang, S.J., Chen, J.L., Mu, X., Zhou, Z.H.: Cost-effective active learning from diverse labelers. In: IJCAI, pp. 1879–1885 (2017)
- [18] Kingma, D.P., Ba, J.: Adam: A method for stochastic optimization. In: ICLR (Poster) (2015)
- [19] Kumar, A., Ma, T., Liang, P.: Understanding self-training for gradual domain adaptation. In: International Conference on Machine Learning, pp. 5468–5479. PMLR (2020)
- [20] Li, S., Kirby, R.M., Zhe, S.: Deep multi-fidelity active learning of high-dimensional outputs. *CoRR* **abs/2012.00901** (2020). URL <https://arxiv.org/abs/2012.00901>
- [21] Li, S., Xing, W., Kirby, R., Zhe, S.: Multi-fidelity bayesian optimization via deep neural networks. *Advances in Neural Information Processing Systems* **33** (2020)
- [22] Mansour, Y., Mohri, M., Rostamizadeh, A.: Domain adaptation: Learning bounds and algorithms. *arXiv preprint arXiv:0902.3430* (2009)
- [23] de Mathelin, A., Deheeger, F., Mougeot, M., Vayatis, N.: Discrepancy-based active learning for domain adaptation. *arXiv preprint arXiv:2103.03757* (2021)
- [24] Pan, Z., Yu, W., Yi, X., Khan, A., Yuan, F., Zheng, Y.: Recent progress on generative adversarial networks (gans): A survey. *IEEE Access* **7**, 36,322–36,333 (2019)
- [25] Papamakarios, G., Nalisnick, E., Rezende, D.J., Mohamed, S., Lakshminarayanan, B.: Normalizing flows for probabilistic modeling and inference. *Journal of Machine Learning Research* **22**(57), 1–64 (2021)
- [26] Peherstorfer, B., Willcox, K., Gunzburger, M.: Optimal model management for multi-fidelity monte carlo estimation. *SIAM Journal on Scientific Computing* **38**(5), A3163–A3194 (2016)
- [27] Peherstorfer, B., Willcox, K., Gunzburger, M.: Survey of multifidelity methods in uncertainty propagation, inference, and optimization. *Siam Review* **60**(3), 550–591 (2018)
- [28] Penwarden, M., Zhe, S., Narayan, A., Kirby, R.M.: Multifidelity modeling for physics-informed neural networks (pinns). *Journal of Computational Physics* p. 110844 (2021)
- [29] Pöltz, C.: Distance based active learning for domain adaptation. In: ICPRAM (2015)

- [30] Prabhu, V., Chandrasekaran, A., Saenko, K., Hoffman, J.: Active domain adaptation via clustering uncertainty-weighted embeddings. In: Proceedings of the IEEE/CVF International Conference on Computer Vision, pp. 8505–8514 (2021)
- [31] Rai, P., Saha, A., Daumé III, H., Venkatasubramanian, S.: Domain adaptation meets active learning. In: Proceedings of the NAACL HLT 2010 Workshop on Active Learning for Natural Language Processing, pp. 27–32 (2010)
- [32] Ramirez-Loaiza, M.E., Sharma, M., Kumar, G., Bilgic, M.: Active learning: an empirical study of common baselines. *Data mining and knowledge discovery* **31**(2), 287–313 (2017)
- [33] Redko, I., Morvant, E., Habrard, A., Sebban, M., Bennani, Y.: A survey on domain adaptation theory: learning bounds and theoretical guarantees. *arXiv preprint arXiv:2004.11829* (2020)
- [34] Rodriguez-Lujan, I., Fonollosa, J., Vergara, A., Homer, M., Huerta, R.: On the calibration of sensor arrays for pattern recognition using the minimal number of experiments. *Chemometrics and Intelligent Laboratory Systems* **130**, 123–134 (2014)
- [35] Saha, A., Rai, P., Daumé, H., Venkatasubramanian, S., DuVall, S.L.: Active supervised domain adaptation. In: Joint European Conference on Machine Learning and Knowledge Discovery in Databases, pp. 97–112. Springer (2011)
- [36] Sarkar, S., Joly, M., Perdikaris, P.: Multi-fidelity learning with heterogeneous domains
- [37] Settles, B.: Active Learning. *Synthesis Lectures on Artificial Intelligence and Machine Learning*. Morgan & Claypool Publishers (2012). DOI 10.2200/S00429ED1V01Y201207AIM018. URL <https://doi.org/10.2200/S00429ED1V01Y201207AIM018>
- [38] Su, J.C., Tsai, Y.H., Sohn, K., Liu, B., Maji, S., Chandraker, M.: Active adversarial domain adaptation. In: Proceedings of the IEEE/CVF Winter Conference on Applications of Computer Vision, pp. 739–748 (2020)
- [39] Takeno, S., Fukuoka, H., Tsukada, Y., Koyama, T., Shiga, M., Takeuchi, I., Karasuyama, M.: Multi-fidelity bayesian optimization with max-value entropy search and its parallelization. In: International Conference on Machine Learning, pp. 9334–9345. PMLR (2020)
- [40] Tran, A., Wildey, T., McCann, S.: smf-bo-2cogp: A sequential multi-fidelity constrained bayesian optimization framework for design applications. *Journal of Computing and Information Science in Engineering* **20**(3) (2020)
- [41] Vergara, A., Vembu, S., Ayhan, T., Ryan, M.A., Homer, M.L., Huerta, R.: Chemical gas sensor drift compensation using classifier ensembles. *Sensors and Actuators B: Chemical* **166**, 320–329 (2012)
- [42] Wang, H., He, H., Katabi, D.: Continuously indexed domain adaptation. In: H.D. III, A. Singh (eds.) *Proceedings of the 37th International Conference on Machine Learning, Proceedings of Machine Learning Research*, vol. 119, pp. 9898–9907. PMLR (2020). URL <https://proceedings.mlr.press/v119/wang20h.html>
- [43] Wang, M., Deng, W.: Deep visual domain adaptation: A survey. *Neurocomputing* **312**, 135–153 (2018)

- [44] Wang, Z., Xing, W., Kirby, R., Zhe, S.: Multi-fidelity high-order gaussian processes for physical simulation. In: International Conference on Artificial Intelligence and Statistics, pp. 847–855. PMLR (2021)
- [45] Wilson, G., Cook, D.J.: A survey of unsupervised deep domain adaptation. *ACM Transactions on Intelligent Systems and Technology (TIST)* **11**(5), 1–46 (2020)
- [46] Zhang, Y., Deng, B., Jia, K., Zhang, L.: Gradual domain adaptation via self-training of auxiliary models. *arXiv preprint arXiv:2106.09890* (2021)
- [47] Zhao, H., Des Combes, R.T., Zhang, K., Gordon, G.: On learning invariant representations for domain adaptation. In: International Conference on Machine Learning, pp. 7523–7532. PMLR (2019)
- [48] Zhou, F., Shui, C., Yang, S., Huang, B., Wang, B., Chaib-draa, B.: Discriminative active learning for domain adaptation. *Knowledge-Based Systems* **222**, 106,986 (2021)
- [49] Zhuang, F., Cheng, X., Luo, P., Pan, S.J., He, Q.: Supervised representation learning: Transfer learning with deep autoencoders. In: Twenty-Fourth International Joint Conference on Artificial Intelligence (2015)
- [50] Zhuang, F., Qi, Z., Duan, K., Xi, D., Zhu, Y., Zhu, H., Xiong, H., He, Q.: A comprehensive survey on transfer learning. *Proceedings of the IEEE* **109**(1), 43–76 (2020)